
Article:

Al-Haideri, H., White, M.A. and Kelly, D.J. orcid.org/0000-0002-0770-6845 (2016) Major contribution of the type II beta carbonic anhydrase CanB (Cj0237) to the capnophilic growth phenotype of Campylobacter jejuni. Environmental Microbiology, 18 (2). pp. 721-735. ISSN 1462-2912

https://doi.org/10.1111/1462-2920.13092

---

environmental microbiology
environmental microbiology reports

Major contribution of the type II beta carbonic anhydrase CanB (Cj0237) to the capnophilic growth phenotype of Campylobacter jejuni

Journal:	*Environmental Microbiology and Environmental Microbiology Reports*
Manuscript ID	EMI-2015-1233.R1
Manuscript Type:	EMI - Research article
Journal:	Environmental Microbiology
Date Submitted by the Author:	n/a
Complete List of Authors:	Al-Haideri, Halah; The University of Sheffield, Molecular Biology and Biotechnology White, Michael; The University of Sheffield, Molecular Biology and Biotechnology Kelly, David; The University of Sheffield, Molecular Biology and Biotechnology
Keywords:	bacteria, environmental signal/stress responses, growth and survival, metabolism, metals, microbial genetics, metabolic networks

Major contribution of the type II beta carbonic anhydrase CanB (Cj0237) to the capnophilic growth phenotype of *Campylobacter jejuni*

Halah Al-Haideri [¶], Michael A. White and David J. Kelly*

Department of Molecular Biology and Biotechnology, The University of Sheffield, Firth Court, Western Bank, Sheffield S10 2TN, UK.

[¶] Present address: Department of Biology, College of Science for Women, The University of Baghdad, Baghdad, Iraq.

***Author for correspondence:** Professor D. J. Kelly, tel: +44 114 222 4414; fax: +44 114 272 8697. Email: d.kelly@sheffield.ac.uk

Running title: Role of *Campylobacter jejuni* beta carbonic anhydrase

Key words: Carboxylase, bicarbonate, anaplerotic, zinc, pathogen

Summary

Campylobacter jejuni, the leading cause of human bacterial gastroenteritis, requires low environmental oxygen and high carbon dioxide for optimum growth, but the molecular basis for the carbon dioxide requirement is unclear. One factor may be inefficient conversion of gaseous CO_2 to bicarbonate, the required substrate of various carboxylases. Two putative carbonic anhydrases (CA's) are encoded in the genome of *C. jejuni* strain NCTC 11168 (Cj0229 and Cj0237). Here, we show that deletion of the *cj0237* (*canB*) gene alone prevents growth in complex media at low (1 % v/v) CO_2 and significantly reduces the growth rate at high (5% v/v) CO_2. In minimal media incubated under high CO_2, the *canB* mutant grew on L-aspartate but not on the key C3 compounds L-serine, pyruvate and L-lactate, showing that CanB is crucial in bicarbonate provision for pyruvate carboxylase mediated oxaloacetate synthesis. Nevertheless, purified CanB (a dimeric, anion and acetazolamide sensitive, zinc-containing type II beta-class enzyme) hydrates CO_2 actively only above pH 8 and with a high K_m (~34 mM). At typical cytoplasmic pH values and low CO_2, these kinetic properties might limit intracellular bicarbonate availability. Taken together, our data suggest CanB is a major contributor to the capnophilic growth phenotype of *C. jejuni*.

Introduction

Campylobacteriosis is the most common zoonotic cause of food-borne bacterial enteritis in industrialised countries (Epps *et al*., 2013), predominantly due to *Campylobacter jejuni* infection. These epsilonproteobacteria normally colonise the caeca of wild and domesticated birds and human Infections are predominantly acquired by consumption of contaminated poultry products. In the UK alone, up to 60-80% of retail chicken may be contaminated with *C. jejuni* (Sheppard *et al*., 2009). The human clinical symptoms are typically characterized by bloody diarrhoea, abdominal pain and fever (Allos, 2001). The ability of *C. jejuni* to colonize different hosts and compete against the gut microbiota is due to several colonisation and virulence factors such as motility and chemotaxis, adhesion and invasion, the production of toxins and the ability to acquire key nutrients for growth (Hermans *et al*., 2011). Understanding the physiology of growth in both avian and mammalian hosts, as well as survival in the food chain, will be key to interventions aimed at reducing the medical and economic burden of campylobacteriosis.

Our knowledge of the metabolism of *C. jejuni* has grown in recent years, due to the availability of multiple genome sequences, coupled with both genome-wide and gene-specific functional and biochemical studies (recently reviewed by Stahl *et al*., 2012 and Hofreuter, 2014). *C. jejuni* has a restricted pattern of carbohydrate catabolism; in particular it lacks the ability to use most common sugars as carbon sources. The genome sequences of various *C. jejuni* strains reveal the absence of common sugar transporters and phospofructokinase, which is required for the phosphorylation of fructose-6-phosphate during glycolysis (Parkhill *et al*., 2000, Velayudhan and Kelly, 2002). All of the other Embden-Meyerhof pathway enzymes are present, which thus function in reverse for gluconeogenesis. However, Muraoka and Zhang, (2011) and Stahl *et al*. (2011), demonstrated that some *C. jejuni* strains, such as NCTC11168 are able to transport and catabolise L-fucose via a novel pathway and some *C. jejeuni* subsp. *doylei* and *C. coli* strains can utilise glucose via the Entner-Doudoroff pathway (Vorwerk *et al*., 2015). It is well established, however, that all *C. jejuni* strains are able to catabolise simple organic acids and certain amino-acids (Kelly, 2008). Serine, aspartate, glutamate and proline (and glutamine and asparagine in some strains) are the only amino-acids that support growth of the

majority of strains as sole C-sources (Velayudhan *et al*., 2004, Guccione *et al*. 2008, Hofreuter *et al*. 2008). Mutants lacking the ability to transport or catabolise these amino-acids show colonisation defects in avian and mammalian hosts (Velayudhan *et al*., 2004, Guccione *et al*., 2008; Hofreuter *et al*., 2008, 2012) underlining their *in vivo* importance.

Unlike many other enteropathogens, *C. jejuni* is microaerophilic and requires a gas atmosphere containing lowered levels of oxygen for growth (generally in the range of 5-10% v/v oxygen in the gas atmosphere), although the aerotolerance of different strains varies significantly (Bolton and Coates, 1983). A major mechanism for oxygen mediated growth inhibition is the oxidative lability of key iron-sulphur cluster containing enzymes used by *C. jejuni* in central metabolism, particularly the pyruvate and 2-oxoglutarate oxidoreductases (POR and OOR), which are more typically found in anaerobes (Kendall *et al*., 2014). However, optimal growth of *C. jejuni* also requires elevated carbon dioxide levels (Bolton and Coates, 1983) and the bacterium is therefore classified as capnophilic as well as microaerophilic. There is a complex and poorly understood inter-relationship between the oxygen and carbon dioxide requirements of campylobacters, in that it is possible to ameliorate the oxygen inhibition of growth by the inclusion of high carbon dioxide concentrations in the gas atmosphere (Bolton and Coates, 1983; Fraser *et al*., 1992), but the physiological reasons for the enhanced carbon dioxide requirement for the growth of *C. jejuni* and some other epsilonproteobacteria are not clear. Although it has been shown *in vitro* that low rates of CO_2 fixation might occur through a reversal of the POR and OOR reactions in *H. pylori* and *C. jejuni* cell extracts (St Maurice *et al*., 2007), this seems unlikely to form the basis of a physiologically relevant autotrophic carbon fixation pathway *in vivo.*

A well-known biochemical role for CO_2 in heterotrophic bacteria is in anabolic or anaplerotic reactions, but the carboxylation enzymes involved often specifically require bicarbonate rather than CO_2 as a substrate. The rate of the spontaneous hydration of CO_2 to bicarbonate is slow and adequate provision of intracellular bicarbonate for such enzymes is aided by the operation of carbonic anhydrases (CA's). These metalloenzymes are widely distributed in all kingdoms of life and catalyse the reversible hydration of CO_2 to bicarbonate and protons (Smith and

Ferry, 2000). They play many metabolic roles in both prokaroytes and eukaryotes and can be divided into at least six phylogenetic groups, designated as the α, β, γ, δ, ζ and η-classes (Smith and Ferry, 2000, Supuran, 2008, Ozensoy Guler *et al*. 2015). The α-class carbonic anhydrases are widely distributed in mammals, protozoa, fungi, algae, some prokaryotes and the plant cytoplasm, whereas the β-class can be found in bacteria, fungi, algae and plant chloroplasts. The γ class are also found commonly in the domains *Bacteria* and *Archaea*, and both the δ and ζ classes are common in marine diatoms (Smith and Ferry, 2000, Supuran 2011). The different CA classes have arisen by convergent evolution and are distinct in their secondary, tertiary and quaternary structures; the enzymes belonging to the α-class are usually monomeric, β-CA enzymes are oligomeric with 2-8 monomers and γ-CA enzymes are homotrimers (Smith and Ferry, 2000). In addition, they exhibit differences in their active sites, as both α and β classes require a single Zn^{2+} ion for their catalytic activity, whereas, the γ-class may require Zn^{2+}, Fe^{2+} or Co^{2+}, and the ζ-class may use Cd^{2+} for catalytic activity (Osenzoy Guler *et al*. 2015). Despite these differences, all CA's exhibit a similar mechanism based on divalent metal ion dependent deprotonation of water, resulting in formation of a hydroxide ion. In this mechanism, CO_2 is converted into bicarbonate when the hydroxide ion initiates nucleophilic attack on the carbonyl group of CO_2 (Cronk *et al*., 2001).

Strains of *C. jejuni* encode two unrelated putative CA's of the gamma and beta classes with unknown roles (Smith and Ferry, 2000). Here, we show that growth under low CO_2 conditions is dependent on the *cj0237* (*canB*) gene, encoding the beta-class CA. In minimal media, lack of CanB prevents growth on the key C3 compounds L-serine, pyruvate and L-lactate as sole C-sources but growth does occur with the C4 amino-acid L-aspartate. Thus, one crucial physiological role for CanB is in bicarbonate provision for oxaloacetate synthesis, which in *C. jejuni* occurs exclusively via pyruvate carboxylase (Velayudhan and Kelly, 2002). CanB was heterologously expressed and purified and shown to be a dimeric, zinc-containing type II beta-class enzyme that hydrates CO_2 with low affinity and is most active only above pH 8. The phenotypes of the *canB* deletion mutant and the properties of the enzyme demonstrate that CanB has a key role in the microaerobic physiology of *C. jejuni* and contributes to its capnophilic phenotype. Finally, although CanB was

inhibited by the classical CA inhibitor acetazolamide (AZ), cellular growth at low CO_2 was fairly resistant to this compound.

Results

Bioinformatic and structural analysis of two putative carbonic anhydrases in C. jejuni

The *cj0229* and *cj0237* genes in strain NCTC 11168 encode two unrelated putative CA's of the gamma and beta classes respectively (Parkhill *et al*., 2000; Smith and Ferry, 2000). *cj0229* is located just downstream of the *arg* gene cluster, as first identified by Hani *et al*. (1999). Cj0229 is annotated as an acetyltransferase and CA-like protein (Gundogdu *et al*. 2007). An alignment of the primary sequence with the prototypical gamma CA from *Methanosarcina thermophila* (Cam; Alber and Ferry, 1994; Ferry, 2010) shows three conserved histidine residues (H64, H93 and H98 in Cj0229), which are known to be involved in metal binding in the archaeal protein. However, residues essential for CA activity in Cam (Glu62, Glu84 and Asn202; Ferry, 2010) are not conserved in Cj0229, suggesting it may not be able to hydrate CO_2. Sequence comparisons revealed that Cj0229 also shares significant amino-acid identity with ferripyochelin-binding proteins (Sokol and Woods, 1983), with CaiE, necessary for carnitine utilisation in *E. coli* (Eichler et al., 1994) and with PaaY, involved in phenylacetate degradation in *E. coli* (Fernandez *et al*., 2014). A PHYRE[2] model (Kelley *et al*., 2015) of the predicted tertiary structure of Cj0229 revealed a coiled N-terminal domain formed by a left-handed parallel β-helix (Fig. 1a), typical of the gamma class of CA's, in which the metal binding histidine residues are located at the monomer interfaces of a trimer (Ferry, 2010). BLAST searches show that Cj0229 is highly conserved amongst sequenced *C. jejuni* strains and has homologues in a range of other epsilonproteobacteria.

Examination of the 211 amino-acid sequence of Cj0237 shows that it possesses the two conserved cysteines (C39 and C103), aspartate (D41), arginine (R43) and a histidine (H100) characteristic of the β-class of CA's, which bind a zinc ion at the active site (Fig. 1b). In addition, G55 is a conserved residue that is involved in formation of the dimer interface in other bacterial beta-CA's (Lotlikar *et al*., 2013). BLAST searches show Cj0237 homologues to be highly conserved amongst

sequenced strains of *C. jejuni, C. coli* and most other epsilonproteobacteria. Although Cj0327 is currently designated as CynT (Parkhill *et al*., 2000; Gundogdu *et al*., 2007) due to sequence similarity with the *E. coli* CynT CA enzyme, phylogenetic analysis shows that Cj0237 and *E. coli* CynT reside in different clades of the beta class of CA's (Smith and Ferry, 2000). Moreover, the *cyn* operon in *E. coli* encodes enzymes specialised for cyanate degradation, in which CynT plays a key role (Guillotin *et al*., 1992). *E. coli* does, however, contain an additional beta class CA, designated Can (formerly YadF or confusingly "CynT2"), which is in the same phylogenetic clade as Cj0237 (Smith and Ferry, 2000). Structural modelling of Cj0237 was carried out using the PHYRE[2] server (Fig. 1c). The top five template hits with 95-98% coverage (27-34% sequence identity) included several plant-derived beta CA enzymes and the *E. coli* Can enzyme. Fig. 1c shows the excellent superposition of the Cj0237 model with the determined *E. coli* Can structure. Given that Cj0237 is structurally and phylogenetically most similar to Can and not CynT, we suggest Cj0237 is re-designated as CanB (for carbonic anhydrase beta class) and we will use this designation hereafter.

Expression of cj0229 *and* canB *at different environmental CO_2 levels*

The gene organisation in the *cj0229-cj0237* region of strain NCTC 11168 is shown in Fig. 2a. *cj0229* is monocistronic and divergently oriented with respect to Cj0228c, encoding a protein-L-isoaspartate O-methyltransferase. A previous RNAseq study (Dugar *et al*., 2013) provided no evidence that *cj0229* was transcribed in several strains of *C. jejuni*. However, RT-PCR with internal *cj0229* primers (Fig. 2b) clearly showed expression of the gene in our NCTC 11168 strain. Interestingly, we noted from the genome sequence that *canB* (*cj0237*) is translationally coupled to *cj0238*, encoding MscS, a small mechanosensitive ion channel (Kakuda *et al*., 2012) and we confirmed by RT-PCR that these genes are co-transcribed (Fig. 2b).

A comparison of the expression levels of the *cj0229* and *canB* genes was performed by qRT-PCR in shaken MHS broth cultures under two different CO_2 conditions but identical oxygen concentrations. The low CO_2 condition was 1% (v/v), while 5% (v/v) was used as the higher CO_2 condition, as this is widely employed in microaerobic gas mixtures in many laboratories for routine *C. jejuni* growth. qRT-PCR performed on RNA from mid-log phase cells showed no significant difference in the expression

of *canB* at low or high CO_2, while the expression of *cj0229* was slightly reduced under low CO_2 conditions (Fig. 2c).

CanB is required for normal growth in complex media at low environmental CO_2 levels and for growth on C3 compounds

The effect of deleting *canB* on the growth of *C. jejuni* NCTC 11168 was monitored at low (1% v/v) and high (5% v/v) CO_2 conditions. Figure 3 compares the growth of wild type, *canB* and a complemented strain under these two gas atmospheres. In the higher CO_2 atmosphere (Fig. 3a), although the final cell yields of all strains were similar with an OD_{600} of ~1.0, the *canB* mutant showed a slower growth rate than the wild-type, with approximate doubling times of 4 h and 2.5 h respectively. Complementation with the wild-type gene restored the mutant to a similar growth rate to the wild-type (Fig. 3a). Under the low CO_2 (1% v/v) conditions, the wild-type and complemented strain both showed a similar longer doubling time of about 3 h, whereas, the *canB* mutant did not show any significant growth during the experiment (Fig. 3b). These results clearly indicate that CanB plays a vital role in CO_2 homeostasis in *C. jejuni*, especially under low CO_2 conditions.

In order to determine the potential role of CanB in anaplerotic reactions supporting amino-acid biosynthesis, growth assays were performed using modified MCLMAN minimal media (Alazzam *et al*., 2011) under 5% v/v CO_2 microaerobic incubation conditions. Growth of the wild-type and complemented strain on 20 mM L-serine, pyruvate or L-lactate as sole C-sources could be demonstrated in comparison with the control, while the *canB* mutant did not grow significantly above the inoculation level in the presence of any of these substrates (Fig. 4). In contrast, all three strains grew to a similar final cell density when excess L-aspartate was added in addition to L-serine (Fig. 4). These results indicate that CanB is essential for growth of *C. jejuni* on C3 compounds that can be converted to pyruvate, the substrate for pyruvate carboxylase, which is converted to oxaloacetate.

C. jejuni *CanB is a dimeric zinc-containing enzyme*

To study the properties and catalytic activity of the *C. jejuni* CanB carbonic anhydrase, the *canB* gene was cloned in the pET21a(+) vector and expressed in *E.*

coli BL21 (DE3). The ~ 24.8 kDa CanB protein with a C-terminal 6 x his tag was successfully over-produced and purified by nickel affinity chromatography (Fig. 5a). The oligomeric state and metal-ion content of CanB was determined by fast protein liquid chromatography on a calibrated Superdex 200 gel filtration column (Fig. 5b and 5c). A single symmetrical peak of UV absorbing material was eluted, with a peak elution volume of 75.4 ml and K_{av} 0.46 (Fig. 5b), corresponding to a molecular weight of about 48 kDa (Fig. 5d). This result clearly shows that CanB is a dimeric protein in solution. The peak fractions from gel filtration were analyzed by ICP-MS, which revealed a specific correlation of zinc content with the protein profile (Fig. 5c). No other metal ions were detected above background. The determined molar ratio of protein:zinc in the purified protein was calculated to be 1:0.8, which is close to the expected ratio of 1:1 per monomer. Taken together, the above results confirm that CanB belongs to the dimeric β-class of carbonic anhydrases and suggest that Zn^{2+} is the catalytic metal ion.

CanB catalyses CO_2 hydration but has no esterase activity

The most common way of assaying the activity of CA enzymes is by following the pH change associated with either the production or utilisation of protons in the hydration of CO_2 to bicarbonate or in the dehydration of the latter, respectively. There are technical challenges in this assay as the uncatalysed rate of interconversion is significant and (unless a stopped-flow device is employed) the assay usually has to be performed at low temperatures to obtain measurable rates. The difference between uncatalysed and catalysed initial rates of pH change (using absorbance changes of the indicator phenol red) with CO_2 (starting pH 8.3) or bicarbonate (starting pH 6) are shown for the purified CanB enzyme in Fig. 6a. CanB dependent CO_2 hydration activity was clearly evident, whereas the rate of the reverse reaction was hardly increased in the presence of CanB. For the CO_2 hydration reaction an apparent K_m of 34 ± 10 mM was determined by varying the initial CO_2 concentration and measuring the difference between catalysed and uncatalysed rates (Fig. 6b). Many CA's of the alpha class possess significant esterase activity with a range of substrates, but this property has not been reported amongst bacterial beta class CA's to date (Innocenti and Supuran, 2010). In accord with this, we could not detect esterase activity with purified CanB preparations, using p-nitrophenyl acetate (p-NPA) as substrate and bovine CA (Sigma) as a positive control (data not shown).

Given that the purified enzyme readily hydrates CO_2 and we had shown expression of the *canB* gene in *C. jejuni* (Fig. 2), we sought to measure CA activity *in vivo* using the pH indicator method. However, we could not detect CA activity in intact cells or cell-free extracts of strain NCTC 11168 made by either sonication or lysozyme digestion, suggesting this method is not sensitive enough with crude extracts. Similar observations with other bacteria have been reported previously (Kusian *et al*., 2002).

CanB undergoes pH dependent structural changes as revealed by CD spectroscopy and has low activity below pH 8

Beta-class CA enzymes can be divided into two groups based on the co-ordination of the zinc ion at the active site. Irrespective of the ambient pH, type I enzymes have a more open active site conformation, where the catalytic zinc ion is liganded by two Cys, one His and a water molecule. The type II enzymes have a “closed” active site at neutral or lower pH where an Asp residue ligates the zinc instead of water, in addition to the two Cys and one His residue. Type II enzymes are thus not active at pH values <8 because the water molecule necessary for the formation of the nucleophilic hydroxide in the catalytic mechanism is absent (Cronk *et al*., 2001). However, above pH 8, the metal bound water molecule is readily deprotonated, and a nearby Arg residue forms a salt bridge with the Asp, enabling Zn-hydroxide mediated catalysis (Pinard *et al*., 2015). Importantly, this transition can be accompanied by a substantial conformational change, which “opens” the active site above pH 8. As shown in the active site structural model of CanB in Fig. 1c, the requisite Asp-Arg pair is predicted to be in a similar conformation as in the *E. coli* enzyme, so we investigated pH dependent structural and activity changes in *C. jejuni* CanB. Fig. 7a shows the results of far UV-CD spectroscopy performed on purified CanB in phosphate buffer at the same protein concentration but at different pH values below (pH 7.4) and above (pH 8.5) the predicted transition pH. The spectra are typical of a largely alpha-helical protein, with characteristic minima at 208 and 220 nm and a maximum at 190 nm (Kelly *et al*., 2005). There is a clear pH-dependent difference in the mean residue ellipticity at each of these wavelengths (~10% difference at 220 nm), indicative of a significant conformational change, which would be consistent with the opening of the active site above pH 8. The

consequences of such a conformational change for the activity of the enzyme are shown in Fig. 7b and 7c, where a comparison of the catalysed and uncatalysed CO_2 hydration activity was performed at pH 8.5 and pH 7.4. With 0.1 μM purified enzyme, activity was not detectable above the uncatalysed rate at pH 7.4, whereas at pH 8.5 the catalysed rate was rapid. Only with 1 μM enzyme, could some activity be detected at the lower starting pH. Thus, CanB-dependent activity was clearly much lower at pH 7.4, (by a factor of ~20-fold), supporting the view that CanB behaves as a type II beta class enzyme which is most active above pH 8.

Anion inhibition of CanB at pH 8.5

A variety of inorganic anions have been studied as potential inhibitors of CA's, as they bind with varying affinity to the metal ion at the enzyme active site (De Simone and Supuran, 2012). A small anion inhibition study of purified CanB (Fig. 7d) with 0.1 μM enzyme and 1 mM of selected anions (incubated for 15 mins with the enzyme before assaying) showed that azide and nitrite were fairly potent inhibitors (~50% lowering of the uninhibited rate), tungstate and arsenite had a slight effect (~10% inhibition), while selenate caused minimal inhibition at the concentration used. Azide and nitrite inhibition of CanB is a typical pattern also seen with several diverse CA's of various phylogenetic classes (De Simone and Supuran, 2012).

Binding of the sulphonamide drug acetazolamide to CanB and effects on activity and growth

Sulphonamide class drugs are well-known CA inhibitors (Carta *et al*., 2014). Addition of a molar excess of acetazolamide (AZ) to CanB caused a significant quenching of the intrinsic tryptophan fluorescence of the protein (E_m max = 333 nm). With 10 μM AZ added to 0.2 μM CanB, the maximum quench observed was ~15% (Fig. 8a). Titration of the quench clearly showed that AZ was a tight binding inhibitor with an estimated K_d value of ~30 nM (Fig. 8b). Addition of a molar excess of AZ to CanB significantly inhibited the CO_2 hydration activity at pH 8.5 (Fig, 8c). These data suggested that AZ might be a good inhibitor candidate for CanB *in vivo.* Given that we have shown the importance of CanB in growth at low CO_2 by the phenotype of a *canB* deletion mutant (Fig. 2), growth assays were performed with *C. jejuni* NCTC

11168 wild type in the absence and presence of increasing concentrations of AZ, under low (1% v/v) CO_2 concentrations. However, only at the highest concentration used (200 μM) did AZ treated cultures show a significant growth inhibition (Fig. 8d), suggesting the drug may have rather limited permeability properties in *C. jejuni*.

Discussion

Capnophilic bacteria include diverse examples of pathogenic and non-pathogenic strains but molecular mechanisms explaining their CO_2 requirement are lacking. We noted the presence of two potential CA encoding genes in *C. jejuni* strains and in this study, focussed on the physiological function of the beta CA enzyme CanB (Cj0237). Although the expression of *canB* itself was not affected by environmental CO_2 levels, we showed by mutant analysis that CanB has a significant role in CO_2 dependent growth in this capnophilic bacterium. At 5% v/v CO_2 in the gas atmosphere, a *canB* deletion mutant had a significant growth defect but at lower environmental CO_2 concentrations, growth was completely prevented, a phenotype that was rescued in the complemented strain. Studies of CA mutants in a number of non-capnophilic bacteria (e.g. Kusian *et al*., 2002; Merlin *et al*., 2003) have shown various phenotypes in terms of the severity of growth inhibition observed but it is interesting to consider these results in the context of other CA enzymes encoded in the genome. For example, in *E. coli* (Merlin *et al*., 2003) deletion of the *can* gene prevents growth in ambient air, a phenotype reversed by high CO_2, even though this bacterium encodes an additional beta-class CA, CynT, as well as three gamma class CA enzymes (Smith and Ferry, 2000). However, CynT is a cyanate inducible enzyme encoded in the *cyn* operon, and seems to have a primary role in catalysing the hydration of the CO_2 generated by the enzyme cyanase (CynS) in order to prevent depletion of the bicarbonate that is required for cyanate degradation (Guillotin *et al*., 1992). The aerobic pathogen *P. aeruginosa* PA01 has three distinct beta CA enzymes but only one of these, PsCA1, was shown by mutant studies to have a major, though not essential, role in growth in air (Lotlikar *et al*., 2013). Genes for an additional three gamma-class CA like enzymes are also present in *P. aeruginosa* PA01 but their roles have not been investigated.

The essential role for CanB at low CO_2 concentrations in *C. jejuni* argues against a significant contribution of the other putative CA in strain NCTC 11168, Cj0229. Consistent with this, although structural modelling suggests that Cj0229 is a metal-binding gamma class CA-like protein (Fig. 1a), key acidic residues necessary for activity in the archetypal *M. thermophila* enzyme are not conserved. Indeed, within the gamma class there are many other enzymes in which these residues are different and at least some seem to have no demonstrable CA activity (Ferry, 2010). They may thus have evolved other functions. For example, In *E. coli* the CaiE gamma-like enzyme is necessary for carnitine metabolism (Eichler *et al*., 1994) and the PaaY enzyme has aryl-CoA thioesterase activity, which is required for the hydrolysis of antagonist-CoA's during phenylacetate degradation (Fernandez *et al*., 2014). Nevertheless, in *Azospirillum brasilense* it has been shown that a putative gamma CA gene is co-transcribed with *argC* and is induced under high CO_2; a specific role in arginine biosynthesis was suggested (Kaur *et al*., 2010) although this has not been tested experimentally. Interestingly, in *C. jejuni*, *cj0229* is co-located with the *arg* gene cluster but is transcribed separately (Dugar *et al*., 2013). Our gene expression analysis showed only a small difference in *cj0229* transcription at low versus high CO_2, so the physiological role of Cj0229 will clearly need further investigation, particularly to determine if it has any CA activity.

Interestingly, *H. pylori*, a close relative of *C. jejuni* that is also capnophilic, has both alpha and beta-CA enzymes (Stähler *et al*., 2005; Bury-Moné *et al*., 2008), but located in different cellular compartments; the alpha-CA is periplasmic while the beta-CA is cytoplasmic. Unlike *C. jejuni*, *H. pylori* produces large amounts of CO_2 via the urease reaction; a model has been proposed for the role of the periplasmic alpha-CA in urea related pH homeostasis (Marcus *et al*., 2005). Stomach acid causes opening of the proton gated UreI channel, which allows diffusion of urea into the cytoplasm where it is hydrolysed to 2 mol ammonia and 1 mol CO_2 by urease. These products can rapidly diffuse into the periplasm where ammonia can become protonated not only by stomach acid but also by protons resulting from the alpha-CA reaction. The bicarbonate produced in the periplasmic CA reaction helps buffer the pH of the periplasm to about pH 6.1 (Marcus *et al*., 2005). Thus, the alpha-CA is specifically involved in the acid adaptation response of *H. pylori*, which is considered important in its ability to colonise the human stomach, but this enzyme is presumably

not needed by *C. jejuni* since it resides in the pH neutral intestinal mucosa. The role of the beta-CA in *H. pylori* is less clear but is likely to be required for bicarbonate supply for cytoplasmic biosynthetic reactions, as proposed here for *C. jejuni*.

Carboxylation reactions serve a crucial anaplerotic function in heterotrophic bacteria because they allow the synthesis of C4-acids such as oxaloacetate (OAA) from the C3 intermediate pyruvate. The inability of the *C. jejuni canB* mutant to grow in minimal media on pyruvate and the C3 compounds L-serine and L-lactate, which are converted to pyruvate, indicates a key role for CanB in supplying bicarbonate for the synthesis of OAA, which is the direct precursor for aspartate and thus the entire aspartate family of amino-acids, as well as pyrimidine nucleotides. In *C. jejuni*, OAA seems to be uniquely synthesised from pyruvate by the ATP and biotin dependent enzyme pyruvate carboxylase (PYC) (Velayudhan and Kelly, 2002). PYC specifically uses bicarbonate in its reaction mechanism; the first step in catalysis is the activation of bicarbonate by ATP to form a carboxyphosphate intermediate, which is used to carboxylate enzyme-bound biotin. Carboxybiotin then reacts with the enol form of pyruvate to form OAA (Jitrapakdee *et al*., 2008; Menefee and Zeczycki, 2014). Mutant studies showed that PYC activity is required to support the growth of *C. jejuni* on C3 compounds like pyruvate or lactate as sole C-source, consistent with a unique role for this enzyme in OAA synthesis, while the other carboxylases phosphoenolpyruvate carboxykinase and malic enzyme are involved in gluconeogenesis (Velayudhan and Kelly, 2002). The identical phenotype of the *canB* mutant (this study) and *pycA* mutant (Velayudhan and Kelly, 2002) in minimal media thus supports a close metabolic relationship between CanB and PYC. However, it is clear that this cannot be the only role of CanB because even in complex MHS media which contains a range of amino-acids including aspartate, growth of the mutant is compromised, particularly at low CO_2. Several other key anabolic reactions require bicarbonate and chief amongst these is fatty acid biosynthesis, involving the carboxylation of acetyl-CoA as the first committed step, catalysed by the biotin dependent acetyl-CoA carboxylase. We cannot exclude that there are also additional physiological roles for CanB. In particular, the transcriptional and translational coupling of *canB* and *mscS* (Fig. 2) strongly suggests a functional interaction of the gene products. *mscS* encodes a mechanosensitive ion-channel that is known to be required in *C. jejuni* for cell survival following osmotic downshock (Kakuda *et al*.,

2012). Intriguingly, in higher organisms, binding of CA to aquaporins has been shown to enhance channel activity (Vilas et al., 2015), which may point to the possibility of modulation of MscS activity by CanB.

Purified CanB proved to be a dimeric zinc-containing enzyme consistent with its sequence based classification as a beta-class CA. The hydration of CO_2 was easily demonstrated using pH indicator assays, but the enzyme did not catalyse the reverse reaction when assayed at an initial starting pH of 6, as is required to measure the increase of pH accompanying the dehydration of bicarbonate. In fact, the hydration of CO_2 was also markedly pH dependent, a feature associated in some other beta-class CA enzymes with structural changes in the active site that result in the formation of an Arg-Asp salt bridge above pH 8, facilitating the zinc-hydroxide catalytically competent state (Cronk *et al*., 2001, 2006; Pinard *et al*., 2015). Modelling suggested that the conserved Arg and Asp residues in the *C. jejuni* CanB are in a similar orientation as in the *E. coli* enzyme, where this change was first described (Cronk *et al*., 2001). Accordingly, we obtained evidence for a marked pH dependent conformational change in CanB by CD spectroscopy which, taken together with the low activity at pH 7.4 compared with pH 8.5, would be consistent with this proposed mechanism and classifies CanB as a type II CA. Circular dichroism is clearly a useful tool in this regard and has recently been used in *P. aeruginosa* to reveal that two out of the three beta-class CA enzymes in this pathogen exhibited pH dependent changes, which correlated with their activity profiles, while in contrast the PsCA1 enzyme was very active at both pH 7.5 and pH 8.3 and did not show any change in its CD spectrum at low and high pH (Lotlikar *et al*., 2013). More recent structural studies of the PsCA3 enzyme confirmed its type II active site geometry and reaction mechanism (Pinard *et al*., 2015).

CanB is the first enzyme identified in *C. jejuni* that is specifically required for growth with CO_2. However, the steep pH dependence of CanB (and type II CA's in general) may have important physiological consequences when considered alongside the quite high K_m value we found of ~34 mM for CO_2. The average cytoplasmic pH of *C. jejuni* is not known, but for *E. coli* growing at neutral external pH it has been estimated to be in the range of 7.5-7.6 (Wilks and Slonczewski, 2007). At such pH values, CanB may have limited activity *in vivo*. In addition, the solubility of CO_2 will

depend on the temperature and gas partial pressure, according to Henry's Law. At the host temperature of 37 °C (mammalian) or 42 °C (avian), the maximum solubility of CO_2 can be calculated to be about 22 mM in water (and somewhat less in the solute containing mucus of the intestine where the bacteria are growing), i.e potentially less than the K_m value of the enzyme (albeit we measured this at low temperature). As there is no evidence that CanB is a highly abundant enzyme in *C. jejuni* (and indeed we could not detect its activity in crude cell-free extracts), the above considerations imply that intracellular bicarbonate provision may well become limited during growth *in vivo* and might be one reason why elevated extracellular CO_2 levels are important for *C. jejuni* proliferation. Other factors such as adequate zinc assimilation (Gielda and DiRita, 2012) may also influence CanB activity *in vivo*.

Finally, in a range of pathogens, the use of sulphonamides or other drugs that inhibit CA's have been proposed as novel anti-infective agents (Capasso and Supuran, 2015) and there are many structurally diverse variants which prevent CO_2 hydration in *in vitro* inhibition studies and that can inhibit bacterial growth (Supuran *et al*., 2003; Capasso and Supuran, 2015). We investigated the interaction of the classical CA inhibitor acetazolamide with the *C. jejuni* CanB enzyme. Binding of AZ could be demonstrated by quenching of the intrinsic tryptophan fluorescence; titration suggested a low K_d value, as has been found with many other types of CA. Although AZ also inhibited the activity of the enzyme *in vitro,* the growth of *C. jejuni* at low CO_2 was rather resistant to the compound (Fig. 8), compared, for example, with *P. aeruginosa* where 200 μM AZ resulted in severe growth inhibition (Pinard *et al*., 2015). It is not clear how AZ gains access to the cytoplasm in intact cells, but it is presumably actively transported across the cytoplasmic membrane and this might simply be inefficient in *C. jejuni*; other CA inhibitors might be found that are more permeable. Although *C. jejuni* growth in either avian or mammalian hosts occurs under conditions of elevated environmental CO_2, the growth defect of the *canB* deletion mutant even at high CO_2, demonstrated in this study, suggests that inhibition of CA activity *in vivo* might be expected to reduce colonisation fitness. Therefore, CanB might be a druggable target for interventions designed to limit the proliferation of the bacteria in the host. However, the challenge is to ensure adequate selectivity, as although host alpha and bacterial beta CA's are unrelated in

sequence and structure, their mechanism is similar and no inhibitors highly specific for beta CA's alone are currently known (Capasso and Supuran, 2015).

Experimental Procedures

Bacterial strains, media and growth conditions

Campylobacter jejuni strain NCTC 11168 was routinely cultured at 37 ºC under microaerobic conditions (10 % [v/v] O_2, 5% [v/v] CO_2, and 85 % [v/v] N_2) in a MACS-VA500 Microaerobic workstation cabinet (Don Whitley Scientific, Shipley, UK) on Columbia agar plates supplemented with 5 % (v/v) lysed horse blood, and 10 µg ml^{-1} of each amphotericin B and vancomycin. For *C. jejuni* mutant selection, kanamycin or chloramphenicol was added to final concentrations of 50 µg ml^{-1} or 30 µg ml^{-1} respectively. Liquid cultures of *C. jejuni* were grown in Müller-Hinton (MH) broth (Oxoid, UK) supplemented with 20 mM L–serine (MHS) with orbital shaking under the above microaerobic atmosphere. Bacterial growth experiments were performed in either MHS or in MCLMAN minimal media (Alazzam *et al*., 2011). Individual carbon sources were added to the latter media from filter-sterilised stock solutions to a final concentration of 20 mM. Inocula for minimal media were prepared from starter cultures grown for 16 h in MHS; the cells were pelleted by centrifugation and resuspended in the basal minimal media without an added C-source before being added to complete MCLMAN to produce an initial optical density at 600 nm of ~0.1. In specific experiments with low CO_2 concentrations, the MACS cabinet atmosphere was changed to 10 % [v/v] O_2, 1% [v/v] CO_2, and 89 % [v/v] N_2. All bacterial growth experiments were monitored by measurements of OD_{600} against the un-inoculated media as a blank. *E. coli* DH5α and BL21 (DE3) were routinely cultured at 37 ºC under aerobic conditions on Luria Bertani (LB) solid or liquid media (Melford, UK) supplemented with appropriate antibiotics and with shaking at 200-250 rpm.

DNA isolation and manipulation, PCR and cloning

C. jejuni chromosomal DNA was extracted using the Wizard Genomic DNA purification Kit (Promega, UK). Plasmid DNA was isolated using the Qiagen Miniprep Kit (Quiagen, Inc). Standard techniques were employed for cloning, transformation,

preparation and restriction analysis of plasmid DNA from *E. coli*. A proof reading Accuzyme DNA polymerase (Bioline, UK) was used for routine PCR, except for isothermal assembly (ISA) reactions. My Taq Mix (Bioline, UK) was used for colony PCR screening of *C. jejuni* strains and for colony screening after transformation of *E. coli*.

Reverse transcription PCR

C. jejuni broth cultures were grown in triplicate to an OD600 nm of 0.5 under both standard microaerophilic conditions (5 % v/v CO_2) and at 1 % (v/v) CO_2 with the remainder of the gas atmosphere as stated above. RNA was extracted directly from the cultures using the SV total RNA isolation system (Promega) as recommended by the manufacturer. Purified RNA samples were DNAse treated using the Turbo-DNA Free kit (Ambion) to remove any contaminating DNA. The RNA concentration and purity were determined by using a Genova nano micro-volume spectrophotometer (Jenway). The treated RNA samples were matched to 10 ng μl^{-1} in nuclease free water and stored at -80°C. Gene specific primers were designed to amplify 150-300 bp fragments of *gyrA* (internal control; gyrA-RT-F, 5´-ATGCTCTTTGCAGTAACCAAAAAA-3´ and gyrA-RT-R, 5´-GGCCGATTTCACGCACTTTA-3´), *cj0229* (cj0229-RT-F; 5´-TGTGTTTTAAGAGCCGATGT-3´ and cj0229-RT-R 5´-TTACCCTTTGTTACAACGCT'3´) and *cj0237* (cj0237-RT-F, 5´-AGCAAAATCCCCATACTCTT-3´ and cj0237-RT-R, 5´-GCCACAAACGACGATATTTT-3´) All primers were diluted to 25 µM in nuclease free water. Each reaction was carried out in a 20 µl volume in a MicroAmp® 96-well optical reaction plate (ABI prism). Reactions were performed using the Sensifast SYBR Lo-ROX one step kit (Bioline, UK). Each reaction contained 10 µl Sensifast SYBR 2x buffer, 0.2 µl of each primer, 0.2 µl reverse transcriptase, 0.4 µl RNAse inhibitor, 2 µl of matched RNA or DNA template and 7 µl nuclease free water. Each reaction using RNA was repeated in triplicate; reactions using genomic DNA for the standard curve were replicated in duplicate. PCR amplification was carried out in a Stratagene MX3005p thermal cycler (Agilent) at 45°C for 10 min; 95°C for 2 min followed by 40 cycles of 95°C for 20 s; 55°C for 30s and 72°C for 20s. Data was collected with the associated MxPRO QPCR software (Agilent). A standard curve for

each gene was generated using a series of *C. jejuni* genomic DNA dilutions. Gene expression between cultures was calculated as relative to gyrA expression. The data were analysed as described previously (Guccione *et al*., 2008). Semi quantitative one step RT-PCR reactions used the same 10 ng µl-1 matched RNA samples from *C. jejuni* grown under normal (5 % v/v CO_2) conditions with primers Cj0229-RT-F/Cj0229-RT-R and Cj0237-RT-F plus an additional reverse primer to demonstrate co-transcription of *cj0237* and *cj0238* (Cj0238-RT-R, 5´-ATTTTACACCTTGGAGCACA-3´). PCR amplification was performed using the MyTaq One-Step RT-PCR kit (Bioline, UK) in a 10 µl volume. Each reaction contained 5 µl MyTaq One-Step 2x buffer, 0.1 µl of each primer, 0.1 µl reverse transcriptase, 0.2 µl RNAse inhibitor, 1 µl of matched RNA or DNA template and 3.5 µl nuclease free water. The PCR products were visualised on a 2% (w/v) agarose gel.

Construction and complementation of a C. jejuni canB *deletion mutant*

A *C. jejuni cj0237* (*canB*) deletion mutant was generated using ISA cloning (Gibson *et al*., 2009). The DNA fragments and primers were prepared as follows. pGEM3zf(-) was digested with HincII and phosphatase treated prior to purification. The kanamycin resistance cassette (*kan*) from pJMK30 (van Vliet *et al*., 1998) was PCR amplified using kan-F (5´-ATTCTCCTTGGTTCTCATGTTTGACAGCTTAT-3´) and kan-R (5´-GCACACCTTGGCTAGGTACTAAAACAATTCAT-3´) primers. The *cj0237* gene (636 bp) was deleted and replaced by the *kan* cassette, in the following manner. Two DNA fragments comprising 432 bp of the upstream region and including the first 43 bp of the gene (Fragment 1) and 612 bp comprising the last 111 bp of the gene plus the downstream sequence (Fragment 2) were PCR amplified using primers with specific adapter regions to the ends of each fragment, as follows; cj0237 F1-F: 5´-GAGCTCGGTACCCGGGGATCCTCTAGAGTCGCAAAGCAAATAAAAGTCCG-3´; cj0237 F1-R: 5´-GAGCTCGGTACCCGGGGATCCTCTAGAGTCGCAAAGCAAATAAAAGTCCG-3´ and cj0237 F2-F; 5´-GAATTGTTTTAGTACCTAGCCAAGGTGTGCGGAAAAATAGAAGTACATGC-3´,

cj0237 F2-R 5´-AGAATACTCAAGCTTGCATGCCTGCAGGTCGAAGAATTTTGTAAATTTTC-3´. These adaptor sequences were homologous to pGEM3zf(-) (F1-F and F2-R) and the *kan* cassette (F1-R and F2-F) to allow annealing of the single stranded terminal sequences produced after exonuclease treatment. Thus the kanamycin resistance cassette (*kan*) is inserted between the two fragments, which is then inserted into the pGEM3zf(-) termini to create a circular plasmid. In the ISA reaction, the fragments were mixed in equimolar concentration with the *kan* cassette and *Hinc*II digested pGEM3zf(-). ISA reactions were either purified using the Qiaquick PCR purification Kit (Qiagen, UK) or used to directly transform competent *E. coli* DH5α on LB media with appropriate selective antibiotics. The correct ISA construct was confirmed by PCR using either kan-F or kan-R primers with the F1 and F2 fragment primers, and automated DNA sequencing. The resulting pGEM0237kan plasmid was used to transform wild type *C. jejuni* 11168 by electroporation with selection on kanamycin containing Columbia blood agar plates. For complementation, the wild type gene was integrated at the psuedogene locus *cj0046,* using the pCmetK vector with expression driven by the constitutive *metK* promoter (Gaskin *et al*., 2007). The gene was inserted into pCmetK by ISA cloning using the primers pCmetK-0237-F (5´-CATTTTAATGAAAGGACTTTTTCATGGAAAATCTTATTAGCGGTGCG-3´) and pCmetK-0237-R (5´-GATAAATTAAAACGTCTCACATGTCATTGAACTTTCCTATCCCCTG-3´), which were designed with 23 bp adapter regions complementary with the pCmetK vector after digestion with *Esp*I. The completed ISA reaction was transformed into competent *E. coli* DH5α, and the correct construct was identified by colony PCR screening using cj0046-F (5´-GAGCCAATCCTATTTACTCAGCTATG-3´) and cj0046-R (5´-CCAGCCCATAAAAGTAAAAGCGAGAC-3´) primers and confirmed by automated DNA sequencing. The resulting plasmid pCmetK0237 was used to transform the *C. jejuni cj0237* deletion mutant strain by electroporation with selection on chloramphenicol containing blood agar plates.

Over-production, purification and metal analysis of CanB

The pET21a(+) vector was used to over-produce recombinant Cj0237 protein with a C-terminal 6-his tag, under the control of the IPTG inducible T7 promoter. The

cj0237 gene was PCR amplified using Cj0237-OvEx-F (5´-AATATACATATGGAAAATCTTATTAGCGG-3´) and Cj0237-OvEx-R (5´-ATATTACTCGAGTTGAACTTTCCTATCCTG-3´) primers to generate a 636 bp product containing *Nde*I and *Xho*I sites (minus the stop codon) which was cloned into *Nde*I and *Xho*I digested pET21a(+) to form the pET0237 plasmid which was confirmed by automated DNA sequencing (GATE-BIOTECH/Light True, UK). A 1 L culture of *E. coli* BL21 (DE3) harbouring pET0237 was grown aerobically to OD_{600} of 0.6 and induced with 0.4 mM IPTG and incubated aerobically at 25 ˚C for 20 hr. Cells were harvested by centrifugation (14,000 x g, 20 min, 4 ˚C) and resuspended in binding buffer (20 mM sodium phosphate buffer pH 7.4, 0.5 M NaCl, 20 mM Imidazole). Cells were cooled on ice and broken by sonication (4 x 20 sec pulses at a frequency of 16 microns amplitude in a soniprep 150 ultrasonic disintegrator, SANYO). Cell debris was removed by centrifugation (20,000 x g, 30 min, 4 ˚C), and the cell-free extract (CFE) was applied to a 5 ml HisTrap column (GE Healthcare, UK). Bound proteins were eluted over 20 column volumes with a linear gradient of 20-500 mM imidazole in binding buffer. Protein containing fractions were analysed by 12% SDS-PAGE before being dialysed against 20 mM Tris-HCl pH 7.4, concentrated and stored at -20 ˚C. For determination of native molecular weight and zinc content, fractions of purified protein from nickel affinity chromatography were concentrated to 10 mg ml^{-1} applied onto a superdex 200 (1.5 X 60 cm), gel filtration column (GE Healthcare, UK) in 20mM Tris-HCl, pH 7.4, 0.5 M NaCl and eluted in the same buffer. Fractions were collected and stored at -20 °C. The zinc content of fractions was determined by inductively coupled plasma–mass spectrometry (ICP-MS) on an Agilent 4500 machine (Department of Chemistry, The University of Sheffield) and the ratio of zinc:protein calculated using the protein sulphur content determined by ICP-MS on the same samples.

Determination of carbonic anhydrase activity using CO_2 and $KHCO_3$ as substrates

The ability of CanB to catalyse the interconversion reaction between CO_2 and bicarbonate and the kinetics of CO_2 hydration were initially determined using the method described by Gai *et al.,* (2014). Purified CanB was diluted in assay buffer (50 mM HEPES, 50 mM Na_2SO_4, 50 mM $MgSO_2$, 0.004%(v/w) phenol red), pH 8.3 for assay using CO_2 as a substrate and pH 6.0 for assay using $KHCO_3$ as a substrate.

An ice-cold saturated CO_2 in water solution (~70 mM, according to Henry's law) was prepared using dry-ice pellets and final concentrations from 10 to 55 mM were used in the assay. The assay was performed in 1 ml final volume in cuvettes thermostatted at 4 °C and the absorbance at 557 nm was measured for 60 sec after rapidly adding the substrate. Using $KHCO_3$ as a substrate, the activity was determined at 40 mM $KHCO_3$ at pH 6. Similar reactions were carried out with both substrates in the absence of enzyme as a control and the difference between the uncatalysed and catalysed rates determined. The K_m for CO_2 was estimated by fitting to the Michaelis-Menten equation using GraphPad Prism 6 Software. To directly compare progress curves for CO_2 hydration activity at high and low pH, and for inhibition studies, the assay method described by Cronk *et al*. (2001) was used, employing *m*-cresol purple at pH 8.5 (578 nm) or phenol red at pH 7.4 (557 nm). At pH 7.4, the assay mix was 25 mM HEPES, 100 mM Na_2SO_4 and 100 μM phenol red. At pH 8.5 the assay mix was 25 mM TAPS, 100 mM Na_2SO_4, 100 μM *m*-cresol purple. The assay mixtures were made up as 2 x strength and reactions started by adding 0.5 ml CO_2 solution to 0.5 ml assay mix (minus or plus enzyme) in the cuvette. These assays were carried out at 10 °C.

Esterase activity of purified CanB

The ability of CanB to hydrolyse *p*-nitrophenylacetate (p-NPA Sigma-Aldrich, UK) was measured as described by Covarrubias *et al.,* (2005) with modifications. The reaction was initiated by adding p-NPA (final concentration 5mM) to the enzyme solution (2.5 μM) in 50 mM Tris-HCl, pH 7.5. The substrate solution was prepared freshly by dissolving p-NPA in DMSO. The reaction was monitored by the increase in the absorbance at 406 nm at 25 °C using a Shimadzu UV-Vis spectrophotometer. To control for the spontaneous hydrolysis of p-NPA, the enzyme was replaced by bovine serum albumen (BSA) in identical reaction conditions. Bovine carbonic anhydrase (Sigma-Aldrich, UK) was used as a positive control.

Fluorescence spectroscopy

Intrinsic tryptophan fluorescence of CanB was measured with a Cary Eclipse fluorimeter (Varian Ltd, UK). Samples (3 ml total volume; 0.2 μM final protein concentration in 50 mM Tris-HCl buffer pH 8) were excited at 280nm (5 nm slit width)

and the emission recorded between 300-400 nm (20 nm slit width). The concentration dependence of the fluorescence quench at 333 nm induced by binding of acetazolamide was monitored after addition of small aliquots of ligand and correcting for dilution. Reactions were performed at 25 °C.

Circular dichroism spectroscopy

Far UV CD spectroscopy was performed with a Jasco J-810 spectropolarimeter operating at 25 °C at 50 nm min^{-1} scan speed from 190-260 nm with 4 s averaging time/point, 1 nm band pass and with a 0.1 cm path length. The CD spectrum of the purified CanB protein was determined at 9 μM final concentration in 20 mM potassium phosphate buffer at either pH 7.4 or 8.5. In far UV CD, the repeating unit is the peptide bond, so the determined ellipticity was converted to the mean residue ellipticity, $[\Theta]_{MRW}$, using a mean residue weight (MRW) value of 114 for his-tagged CanB (MRW = molecular mass/N-1, where N = number of residues) and the equation:

$$[\Theta]_{MRW} = \frac{MRW \times \Theta_{obs}}{10 \times d \times c}$$

Where the Θ_{obs} is the observed ellipticity in degrees, d is the path length in cm and c is the protein concentration in g ml^{-1}, according to Kelly *et al*. (2005). All calculations were performed using Microsoft Excel, and the final data plotted in Graphpad prism.

Acknowledgments

HA-H was supported by a scholarship from the Iraqi government. MAW was supported by a University of Sheffield Ph.D studentship. We thank Svetlana Sedelnikova for help with gel filtration, Rosie Staniforth for assistance with CD spectroscopy and Claudine Bisson for help with rendering of the CanB structural model.

References

Alazzam, B., Bonnassie-Rouxin, S., Dufour, V. and Ermel, G. (2011). MCLMAN, a new minimal medium for *Campylobacter jejuni* NCTC11168. *Res Microbiol* **162**: 173-179.

Alber, B. E. and Ferry, J. G. (1994). A carbonic anhydrase from the archaeon *Methanosarcina thermophila*. *Proc. Natl Acad Aci USA* **91:** 6909-6913.

Allos, B. M. (2001). *Campylobacter jejuni* infections: update on emerging issues and trends. *Clin Infect Dis* **32**: 1201-1206.

Bolton, F. J. and Coates, D. (1983). A study of the oxygen and carbon dioxide requirements of thermophilic campylobacters. *J Clin Pathol* **36:** *829-834.*

Bury-Moné, S., Mendz, G. L., Ball, G. E., Thibonnier, M., Stingl, K., Ecobichon, C. *et al*. (2008). Roles of α and β carbonic anhydrases of *Helicobacter pylori* in the urease-dependent response to acidity and in colonization of the murine gastric mucosa. *Infect Immun* **76:** 497-509.

Capasso, C. and Supuran, C. T. (2015). Bacterial, fungal and protozoan carbonic anhydrases as drug targets. *Expert Opin Ther Targets* **1:** 1-16.

Carta, F., Supuran. C. T. and Scozzafava, A. (2014). Sulfonamides and their isosters as carbonic anhydrases inhibitors. *Future Med Chem* **6**: 1149-1165.

Covarrubias, A., Larsson, A. M., Hogbom, M., Lindberg, J., Bergfors, T., Bjorkelid, C.*, et al*. (2005). Structure and function of carbonic anhydrases from *Mycobacterium tuberculosis*. *J. Biol Chem* **280**: 18782-18789.

Cronk, J. D., Endrizzi, J. A., Cronk, M. R., O'neill, J. W. and Zhang K. Y. J. (2001). Crystal structure of *E. coli* β-carbonic anhydrase, an enzyme with an unusual pH-dependent activity. *Prot Sci* **10**: 911-922.

Cronk, J. D., Rowlett, R. S., Zhang, K. Y. J., Tu, C., Endrizzi, J. A., Lee, J. *et al*. (2006). Identification of a novel noncatalytic bicarbonate binding site in eubacterial β-carbonic anhydrase. *Biochemistry* **45:** 4351-4361.

De Simone G. and Supuran C.T. (2012). (In)organic anions as carbonic anhydrase inhibitors. *J Inorg Biochem*. **111:** 117-129.

Dugar, G., Herbiq, A., FÖrstner, K. U., Heidrich, N., Reinhardt, R., Nieselt, K. & Sharma, C. M. (2013). High-resolution transcriptome maps reveal strain-specific regulatory features of multiple *Campylobacter jejuni* isolates. *PLoS Genet* **9:** e100395.

Eichler, K., Bourqis, F., Buchet, A., Kleber, H. P. & Mandrand-Berthelot, M. A. (1994). Molecular characterization of the *cai* operon necessary for carnitine metabolism in *Escherichia coli*. *Mol Microbiol* **13:** 75-86.

Epps, S. V., Harvey, R. B., Hume, M. E., Philips, T.D., Anderson, R. C. and Nisbet, D. J. (2013). Foodborne *Campylobacter*: infections, metabolism, pathogenesis and reservoirs. *Int J Environ Res Public Health* **10**: 6292-6304.

Ferry, J.G. (2010) The γ class of carbonic anhydrases. *Biochim Biophys Acta* **180:** 374-381.

Fernandez, C., Diaz, E. and Garcia, J. L. (2014). Insight on the regulation of the phenylacetate degradation pathway from *Escherichia coli. Environ Microbiol Reports* **6:** 239-250.

Fraser, A. D. E., Chandan, V., Yamazaki, H., Brooks, B. W. and Gracia, M. M. (1992). Simple and economical culture of *Campylobacter jejuni* and *C. coli* in carbon-dioxide in moist air. *Int J Food Infect* **111:** 415-427.

Gaskin, D. H., van Vliet, A. H. M. and Pearson, B. M. (2007). The *Campylobacter* genetic toolbox: development of tractable and generally applicable genetic techniques for *Campylobacter jejuni*. *Zoonoses Public Health* **54**: 101.

Gai, C., Lu, J., Brigham, C. J., Bernardi, A. C. and Sinskey, A. J. (2014). Insights into bacterial CO_2 metabolism revealed by the characterization of four carbonic anhydrases in *Ralstonia eutropha* H16. *AMB Express* **4**: 2.

Gibson, D. G., Young, L., Chuang, R. Y., Venter, J. C., Hutchison, C. A., 3rd and Smith, H. O. (2009). Enzymatic assembly of DNA molecules up to several hundred kilobases. *Nature Methods* **6**: 343-345.

Gielda, L.M. and DiRita, V.J. (2012). Zinc competition among the intestinal microbiota. *MBio* **3:** 00171-12.

Guccione, E., Leon-Kempis, M., Pearson, B. M., Hitchin, E., Mulholand, F., van Diemen, P.M., Stevens, M. P. and Kelly, D. J. (2008). Amino acid-dependent growth of *Campylobacter jejuni*: key roles for aspartase (AspA) under microaerobic and oxygen-limited conditions and identification of AspB (Cj0762), essential for growth on glutamate. *Mol Microbiol* **69**: 77-93.

Guilloton, M. B., Korte, J. J., Lamblin, A. F., Fuchs, J. A. and Anderson, P. M. (1992). Carbonic anhydrase in *Escherichia coli*. A product of the *cyn* operon. *J Biol Chem* **267:** 3731-3734.

Gundogdu, O., Bentley, S. D., Holden, M. T., Parkhill, J., Dorrell, N. and Wren, B. W. (2007). Re-annotation and re-analysis of the *Campylobacter jejuni* NCTC11168 genome sequence. *BMC Genomics* **8:** 162.

Hani, E. K., Ng, D. and Chan, V. L. (1999). Arginine biosynthesis in *Campylobacter jejuni* TGH9011: determination of the *argCOBD* cluster. *Can J Microbiol* **45:** 959-969.

Hermans, D., Deun, K. V., Martel, A., Immerseel, F. V., Messens, W., Heyndrickx, M., Haesebrouck, F. and Pasmans, F. (2011). Colonization factors of *Campylobacter jejuni* in the chicken gut. *Vet Res* **42**: 1-14.

Hofreuter, D., Novik, V. and Galán, J. E. (2008). Metabolic diversity in *Campylobacter jejuni* enhances specific tissue colonization. *Cell Host Microbe* **4**: 425-433.

Hofreuter, D., Mohr, J., Wensel, O., Rademacher, S., Schreiber, K., Schomburg, D., Gao, B. and Galán, J. E. (2012). Contribution of amino acid catabolism to the tissue specific persistence of *Campylobacter jejuni* in a murine colonization model. *PLOS ONE* **7**, e50699.

Hofreuter, D. (2014). Defining the metabolic requirements for the growth and colonization capacity of *Campylobacter jejuni*. *Front Cell Infect Microbiol* **4:** 137.

Innocenti, A. and Supuran, C. S. (2010). Paraoxon, 4-nitrophenyl phosphate and acetate are substrates of α- but not for β-, ɣ- and ζ-carbonic anhydrases. *Bioorganic Med Chem Letters* **20:** 6208-6212.

Jitrapakdee, S., St Maurice, M., Rayment, I., Cleland, W. W., Wallace, J. C. and Attwood, P. V. (2008). Structure, mechanism and regulation of pyruvate carboxylase. *Biochem J* **413:** 369-387.

Kakuda, T., Koide, Y., Sakamoto, A. and Takai, S. (2012). Characterization of two putative mechanosensitive channel proteins of *Campylobacter jejuni* involved in protection against osmotic downshock. *Vet Microbiol*. **160:** 53-60.

Kaur, S., Mishra, M. N. & Tripathi, A. K. (2010). Gene encoding gamma-carbonic anhydrase is cotranscribed with *argC* and induced in response to stationary phase and high CO_2 in *Azospirillum brasilense* Sp7. *BMC Microbiol* **10:** 184.

Kelley, L.A., Mezulis, S., Yates, C.M., Wass, M.N. and Sternberg, M.J.E. (2015) The PHYRE^2 web portal for protein modeling, prediction and analysis. *Nat Protoc* **10:** 848-858.

Kelly, D. J. (2008). Complexity and versatility in the physiology and metabolism of *Campylobacter jejuni.* In: *Campylobacter*. Third edition. Nachamkin, I., Szymanski, C.M.and Blaser, M.J. Eds. ASM Press, Washington D.C.

Kelly, S. M., Jess, T. J. & Price, N. C. (2005) How to study proteins by circular dichroism. *Biochim Biophys Acta* **1751:** 119-139.

Kendall, J. J., Barrero-Tobon, A. M., Hendrixson, D. R. and Kelly, D. J. (2014). Hemerythrins in the microaerophilic bacterium *Campylobacter jejuni* help protect key iron-sulphur cluster enzymes from oxidative damage. *Environ Microbiol* **16:** 1105-1121.

Kusian B., Sültemeyer, D., Bowien, B. (2002). Carbonic anhydrase is essential for growth of *Ralstonia eutropha* at ambient CO_2 concentrations. *J Bacteriol* **184:** 5018-5026.

Lotlikar, S. R., Hnatusko, S., Dickenson, N, E., Choudhari, S., P., Picking, W. L. and Patrauchan, M.A. (2013). Three functional β-carbonic anhydrases in *Psuedomonas aeruginosa* PAO1: role in survival in ambient air. *Microbiology (UK)* **159**: 1748-1759.

Marcus, E. A., Moshfeqh, A. P., Sachs, G. and Scott, D .R. (2005). The periplasmic alpha-carbonic anhydrase activity of *Helicobacter pylori* is essential for acid acclimation. *J Bacteriol* **187**: 729-38.

Menefee, A. L. and Zeczycki, T. N. (2014). Nearly 50 years in the making: defining the catalytic mechanism of the multifunctional enzyme, pyruvate carboxylase. *FEBS J* **281**: 1333-54.

Merlin, C., Masters, M., McAteer, S. and Coulson, A. (2003). Why is carbonic anhydrase essential to *Escherichia coli* ? *J Bacteriol* **185:** 6415-6424.

Muraoka, W. T. and Zhang, Q. (2011). Phenotypic and genotypic evidence for L-fucose utilization by *Campylobacter jejuni*. *J Bacteriol* **139**: 1065-1075.

Ozensoy Guler, O., Capasso, C. and Supuran C. T. (2015). A magnificent enzyme superfamily: carbonic anhydrases, their purification and characterization. *J Enzyme Inhib Med Chem* **29:** 1-6.

Parkhill, J., B. W. Wren, K. Mungall, J. M. Ketley, C. Churcher, D. Basham, T. *et al*. (2000). The genome sequence of the food-borne pathogen *Campylobacter jejuni* reveals hypervariable sequences. *Nature* **403**: 665-668.

Pinard, M. A., Lotlikar, S. R., Boone, C. D., Vullo, D., Supuran, C. T., Patrauchan, M. A. and McKenna, R. (2015). Structure and inhibition studies of a type II beta-carbonic anhydrase psCA3 from *Pseudomonas aeruginosa*. *Bioorg Med Chem* **23:** 4831-4838.

Sheppard, S.K., Dallas, J.F., Strachan, N.J., MacRae, M., McCarthy, N.D., Wilson, D.J. *et al* (2009). *Campylobacter* genotyping to determine the source of human infection. *Clin Infect Dis* **48:** 1072-1078.

Smith, K. S. and Ferry, J. G. (2000). Prokaryotic carbonic anhydrases. *FEMS Microbiol Rev* **24**: 335-366.

Sokol, P. A. and Woods, D. E. (1983). Demonstration of an iron-siderophore-binding protein in the outer membrane of *Psuedomonas aeruginosa*. *Infect Immun* **40:** 665-669.

St Maurice, M. Cremades, N., Croxen, M. A., Sisson, G., Sancho, J. and Hoffman, P. S. (2007). Flavodoxin: quinone reductase (FqrB): a redox partner of pyruvate: ferredoxin oxidoreductase that reversibly couples pyruvate oxidation to NADPH production in *Helicobacter pylori* and *Campylobacter jejuni*. *J Bacteriol* **13:** 4764-4773.

Stahl, M., Friis, L. M., Nothaft, H., Liu, X., Li, J., Szymanski, C. M. and Stintzi, A. (2011). L-Fucose utilization provides *Campylobacter jejuni* with a competitive advantage. *PNAS* **108**: 7194-7199

Stahl, M., Butcher, J. and Stintzi, A. (2012). Nutrient acquisition and metabolism by *Campylobacter jejuni*. *Front Cell Infect Microbiol* **2**: 5.

Stähler, F. N., Ganter, L., Lederer, K., Kist, M. and Bereswill, S. (2005). Mutational analysis of the *Helicobacter pylori* carbonic anhydrases. *FEMS Immun Med Microbiol* **44:** 183-189.

Supuran, C. T., Casini, A. and Scozzafava, A. (2003). Protease inhibitors of the sulfonamide type: anticancer, anti-inflammatory, and antiviral agents. *Med Res Rev* **23:** 535-58.

Supuran, C. T. (2008). Carbonic anhydrase: novel therapeutic applications for inhibition and activators. *Nat Rev Drug Discov* **7**: 168-181.

Supuran, C. T. (2011). Bacterial carbonic anhydrases as drug targets: towards novel antibiotics? *Front Pharmacol* **2**: 1-6.

Vilas, G., Krishnan, D., Loganathan, S.K., Malhotra, D., Liu, L., Beggs, M.R., Gena, P., Calamita, G., Jung, M., Zimmermann, R., Tamma, G., Casey, J.R. and Alexander R.T. (2015) Increased water flux induced by an aquaporin-1/carbonic anhydrase II interaction. *Mol Biol Cell* **26:** 1106-1118.

van Vliet, A. H., Wooldridge, K. G. and Ketley, J. M. (1998). Iron-responsive gene regulation in a *Campylobacter jejuni fur* mutant. *J Bacteriol* **180**: 5291-5298.

Velayudhan, J. and Kelly, D. J. (2002). Analysis of gluconeogenic and anaplerotic enzymes in *Campylobacter jejuni*: an essential role for phosphoenolpyruvate carboxykinase. *Microbiology (UK)* **148**: 685-694.

Velayudhan, J., Jones, M .A. Barrow, P. A. and Kelly, D. J. (2004). L-serine catabolism via an oxygen-labile L-serine dehydratase is essential for colonization of the avain gut by *Campylobacter jejuni*. *Infect Immun* **72:** 260-268.

Vorwerk, H., Huber, C., Mohe, J., Bunk, B., Bhuju, S., Wesel, O. *et al*. (2015). A transferable plasticity region in *Campylobacter coli* allows isolates of an otherwise non-glycolytic food-borne pathogen to catabolize glucose. *Mol Microbiol* doi: 10.1111/mmi. 13159.

Wilks, J. C. and Slonczewski, J. L. (2007). pH of the cytoplasm and periplasm of *Escherichia coli*: rapid measurement by green fluorescent protein fluorimetry. *J Bacteriol* **189:** 5601-5607.

Figure legends

Figure 1. Structural modelling and sequence comparisons of *C. jejuni* CA enzymes. (a) PHYRE[2] model (Kelley *et al*., 2015) of Cj0229, showing the typical left-handed beta coil structure and C-terminal alpha-helix characteristic of the gamma-class of CA enzymes. (b) Sequence alignment of active site residues in selected type II beta class CA's. Key; Cj, *C. jejuni*; Ec, *E. coli* Can (ECCA); Hi, *H. influenzae*; Ps, *P. aeruginosa*. Numbering is for the *C. jejuni* CanB. (c) PHYRE[2] model of *C. jejuni* CanB monomer (cyan) superimposed on the determined structure (grey) of *E. coli* ECCA/Can (PDB code 1I6P; Cronk *et al*., 2001). The boxed region is the active site, shown enlarged with relevant *C. jejuni* CanB residues numbered. The zinc ion is shown as a grey sphere with ligand interactions with amino-acid side chains shown as dotted lines. D41 and R43 are the residues that are predicted to form a salt-bridge at high pH. Figure produced using PyMOL (version 1.5.0.4).

Figure 2. Gene organisation and expression analysis of *cj0229* and *canB*. (a) gene organisation and neighbourhood of the *C. jejuni* NCTC 11168 chromosome containing potential CA encoding genes *cj0229* and *canB* (*cj0237*). The thin arrows above the genes represent the PCR products expected from primers used for RT-PCR reactions in (b) and (c). (b) RNA was isolated from wild type *C. jejuni* 11168 during mid-log phase growth. Internal primers for *cj0229* (cj0229-RT-F/cj0229-RT-R) amplified the predicted 290 bp product by RT-PCR, showing that this gene is expressed in growing cells. A forward primer within *cj0237* (cj0237-RT-F) and a reverse primer within *cj0238* (cj0238-RT-R) amplified the predicted 600 bp product showing that these two genes are co-transcribed. Three PCR reactions were performed using each primer pair, a reverse transcriptase reaction using an RNA template (RT +) and a reverse transcriptase negative reaction using either RNA (RT -) or gDNA templates, acting as negative and positive controls respectively. Lane M; molecular size markers (c) qRT-PCR analysis of gene expression of *cj0229* (using primers cj0229-RT-F/cj0229-RT-R) and *canB* (using primers cj0237-RT-F/cj0327-RT-R) under low (1% v/v) and high (5% v/v) CO_2, with RNA from mid-log phase cultures. The expression at low CO_2 is shown relative to the expression levels normalised to 1.0-fold under 5% v/v CO_2 (the standard *C. jejuni* growth atmosphere). The data shown are the means and SD from three qRT-PCR reactions, each from

three independent cultures grown under 5% v/v or 1% v/v CO_2. Statistical significance was determined by Students t-test (**, p<0.01; NS, not significant).

Figure 3. Comparative microaerobic growth of the *C. jejuni* wild type (solid circles), *canB* mutant (open circles) and complemented *canB* strain (open squares) under 5% v/v CO_2 (a), and 1% v/v CO_2 (b) in the gas atmosphere. *C. jejuni* starter cultures were grown overnight in MHS broth under microaerobic conditions with 5% v/v CO_2, before being inoculated in fresh, prewarmed MHS broth equilibrated overnight with the indicated gas atmospheres. The data points represent the mean ± SEM of at least three independent growth experiments.

Figure 4. Microaerobic growth of wild type, mutant and complemented strain in minimal media with different carbon sources. Starter cultures were grown in overnight in MHS broth, harvested and washed before being inoculated into prewarmed miminal MCLMAN media in shake flasks with the indicated carbon sources at a final concentration of 20 mM each. The initial OD600 was adjusted to 0.1 and the data shown are the means and SEM of wild type (black bars), *canB* mutant (white bars) and the complemented *canB* strain (grey bars) after 24 h growth in a 5% v/v CO_2/ 10% v/v oxygen/ 85% v/v nitrogen atmosphere. The data show the means and SEM of at least four independent growth experiments. The statistical analysis was performed by Students t test with *P< 0.05, **P< 0.01, ***P< 0.001. NS = not significant.

Figure 5. Over-expression and purification of CanB. (a) 12 % SDS-PAGE of expression and purification steps. *E. coli* BL21 (DE3) harbouring pETcanB was grown aerobically to mid exponential phase before being induced with 0.4 mM IPTG. The cells were incubated for 20 h at 25 °C, harvested and a cell-free extract prepared by sonication. CanB was purified by His-trap chromatography before being dialysed against Tris-HCl buffer pH 7.5. Lane M: Prestained Page-ruler Marker proteins (Fisher, UK). Lane 1: *E. coli* BL21 (DE3) (pETcanB) whole cell profile before induction, showing some leaky expression of CanB. Lane 2: whole cell profile after IPTG induction. Lane 3: Clarified soluble cell-free extract loaded on to the His-trap column. Lane 4: Eluted CanB protein with molecular weight of ~24 kDa. (b) Gel filtration chromatography of CanB. A single major eluted peak with an elution volume of 73.5 ml and K_{av} value of 0.457 was observed. (c) 12 % SDS-PAGE of eluted

CanB fractions following gel filtration. Lane 70-78 represents the elution volume. Each fraction was analysed for its zinc content by ICP-MS and is plotted above the gel. (d) Gel filtration calibration curve of CanB. The observed CanB native molecular weight of 48 kDa was determined by reference to standard proteins with known K_{av} values.

Figure 6. CO_2 hydration and bicarbonate dehydration activity of CanB. In (a) the rates of uncatalysed and catalysed CO_2 hydration and $KHCO_3$ dehydration are shown, with 40 mM initial concentration of substrate. The enzyme (0.1 μM) was assayed in a reaction buffer of 50 mM HEPES, 50 mM $MgSO_4$, 50 mm Na_2SO_4, 0.004 % (w/v) phenol red, pH 8.3 with CO_2 as a substrate, and pH 6 for $KHCO_3$ substrate at 4 °C. In (b) the CO_2 concentration was varied at pH 8.3 and the difference between the uncatalysed and catalysed rates determined. The data points represent the mean and SEM of at least six independent assays. The solid curve is the fit to the Michaelis-Menten equation, which gave a K_m of 34 ± 10 mM.

Figure 7. Effect of pH on the structure and activity of CanB and anion inhibition at pH 8.5. (a) Far UV CD spectra of 9 μM CanB in pH 7.4 or pH 8.5 buffer. The change at 222 nm is ~ 10% between the two pH values. (b) CO_2 hydration activity profile measured with *m*-cresol purple at pH 8.5 without (dashed line) and with increasing concentrations of enzyme as indicated. (c) CO_2 hydration activity profile measured with phenol red at pH 7.4 without (dashed line) or with increasing concentrations of enzyme as indicated.. (d) Inhibition of CanB activity by anions, carried out at pH 8.5 with the *m*-cresol purple assay. The enzyme was incubated in assay buffer for 15 min without (dotted line) or with (solid lines) 1 mM of the sodium salts of the anions indicated, before addition of CO_2. In (b)-(d) the reactions were started by addition of freshly prepared saturated CO_2 solution; the initial CO_2 concentration in the assay was ~35 mM.

Figure 8. Interaction of acetazolamide with CanB and effects on activity and growth. (a) Tryptophan fluorescence spectroscopy of acetazolamide binding to CanB, showing the quench at 333 nm induced by addition of 10 μM AZ to 0.2 μM CanB. (b) Fluorescence change at 333 nm over a range of concentrations of AZ with 0.2 μM CanB. The solid line is the fit of the % quench to a one-site binding model, performed in Graph Pad Prism. (c) Effect of AZ on the CO_2 hydration activity of

CanB, measured at pH 8.5 with the *m*-cresol purple assay (see Experimental Procedures). (d) Effect of increasing concentrations of AZ on the growth of *C. jejuni* NCTC 11168 under low CO_2 incubation conditions in MHS media (1% v/v CO_2 in the gas atmosphere). A representative growth experiment from several that were performed is shown.

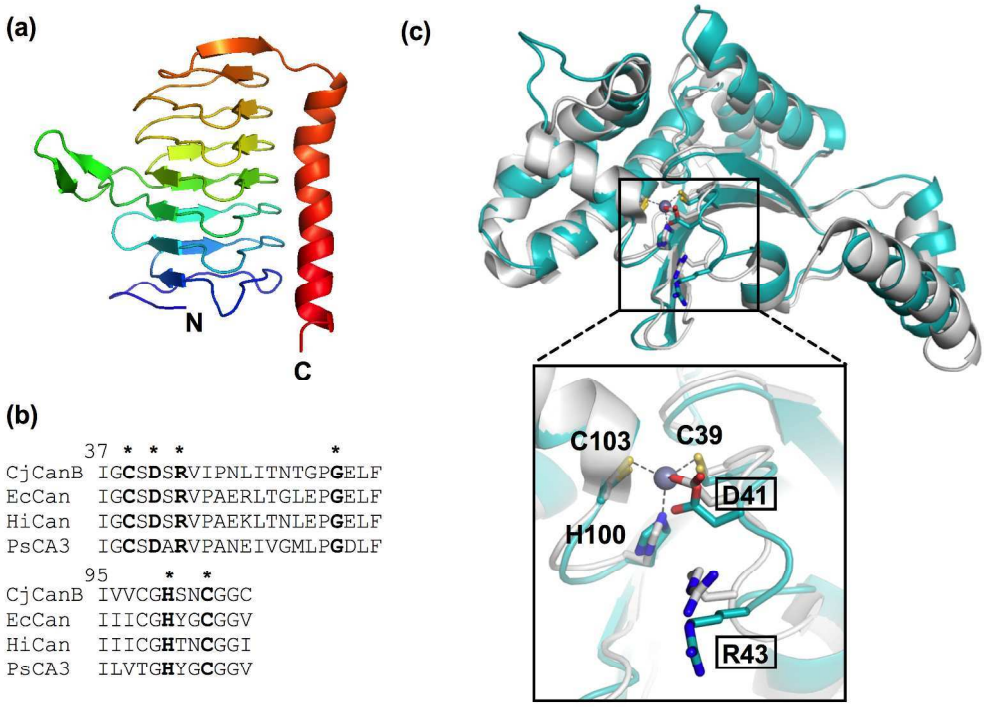

Figure 1
272x208mm (300 x 300 DPI)

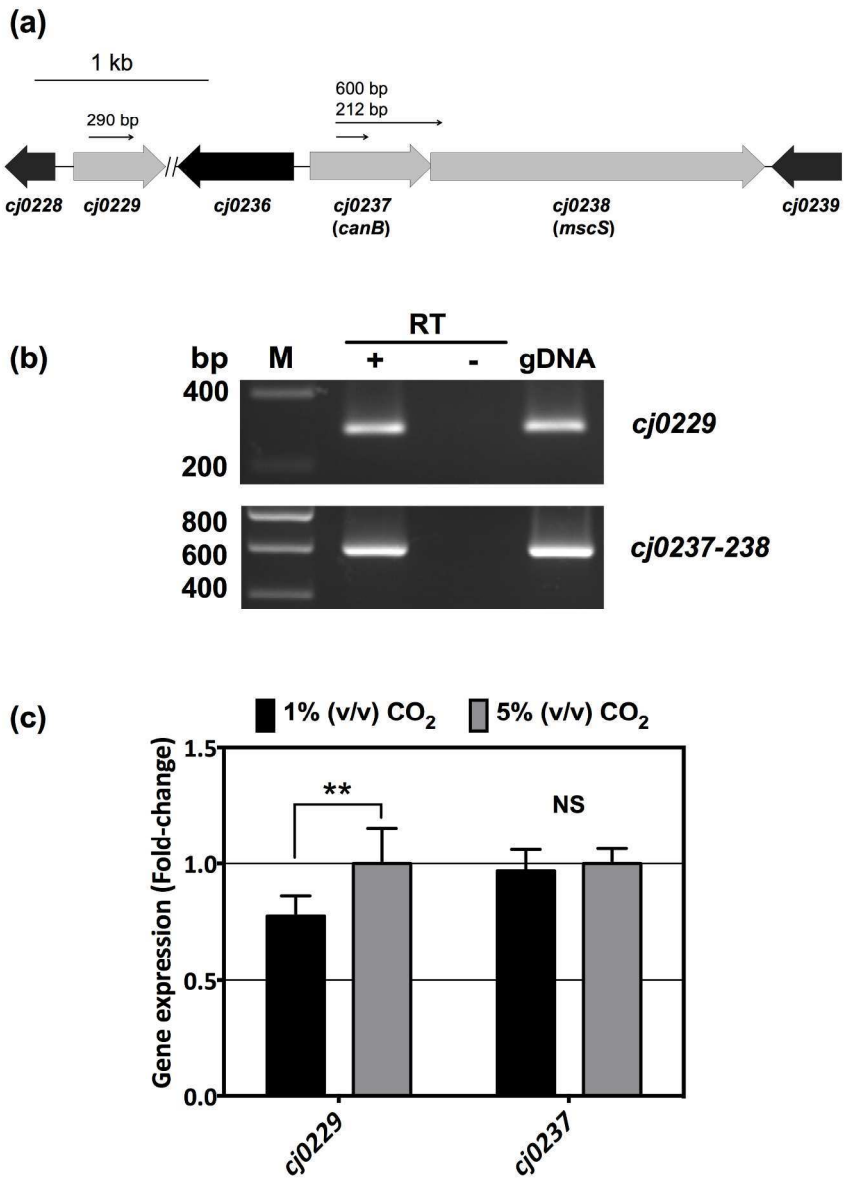

Figure 2
194x271mm (300 x 300 DPI)

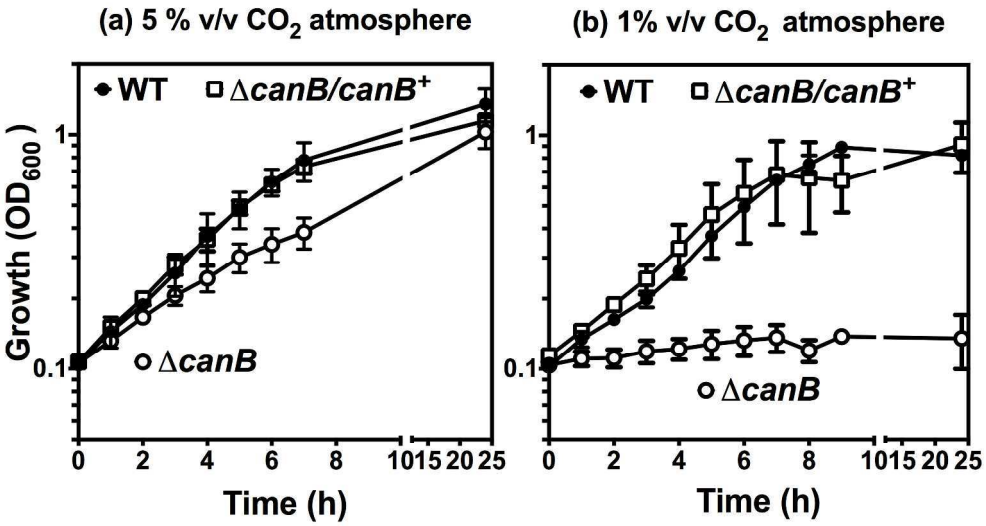

Figure 3
252x136mm (300 x 300 DPI)

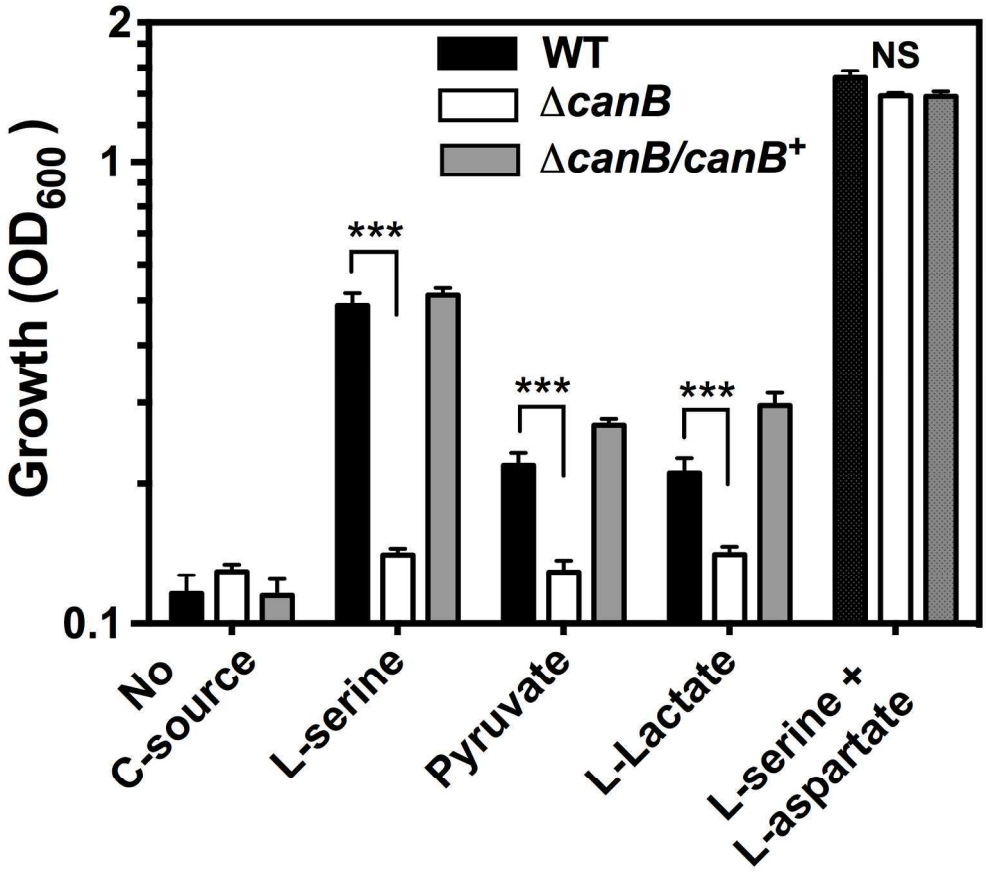

Figure 4
195x177mm (300 x 300 DPI)

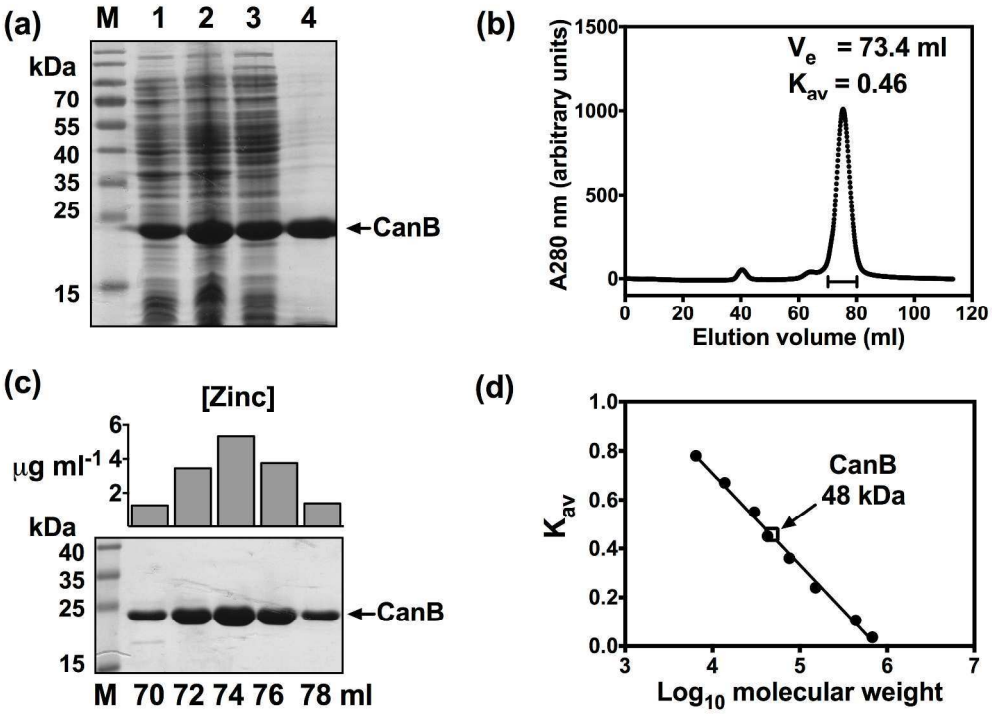

Figure 5
266x194mm (300 x 300 DPI)

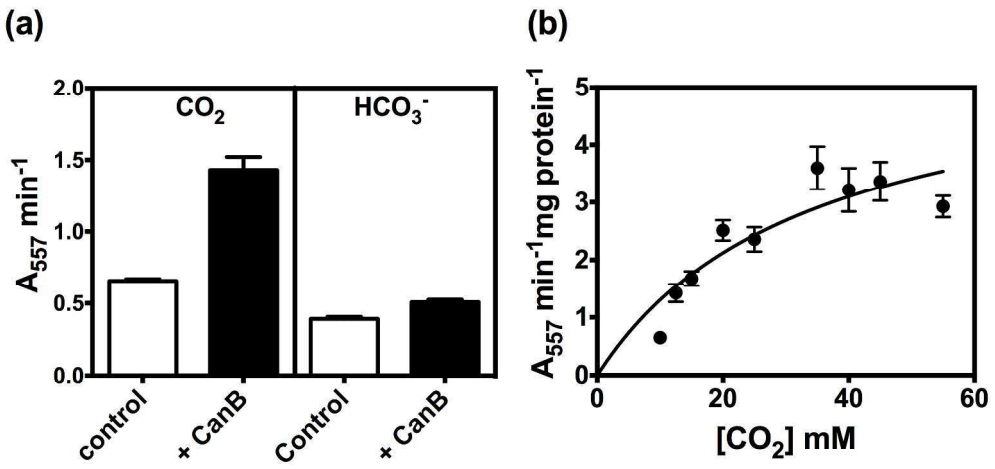

Figure 6
255x122mm (300 x 300 DPI)

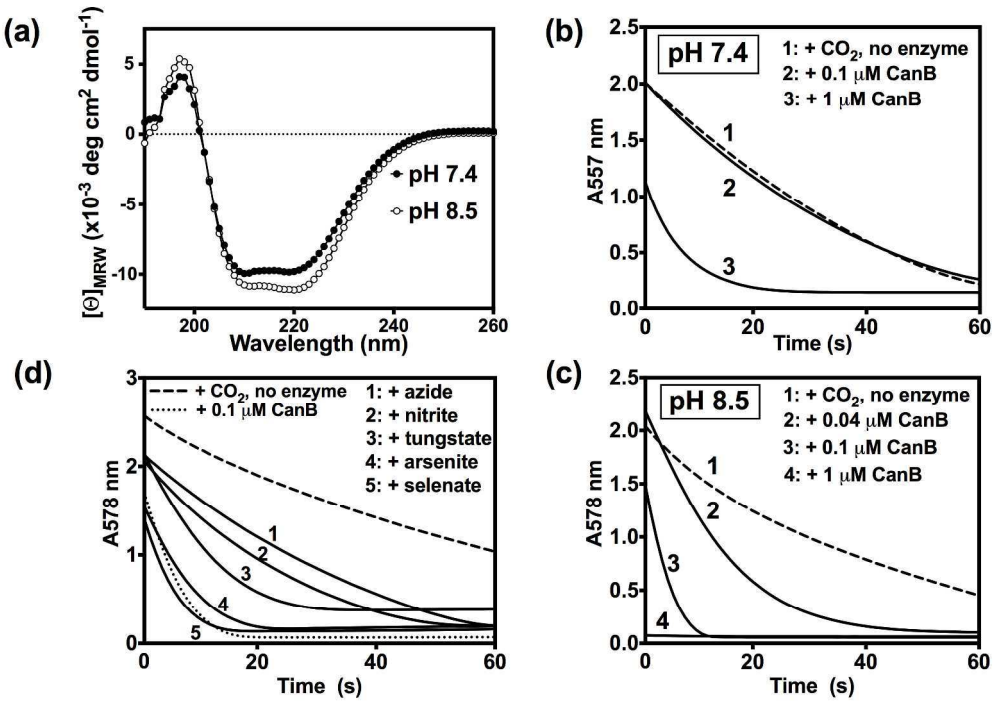

Figure 7
272x193mm (300 x 300 DPI)

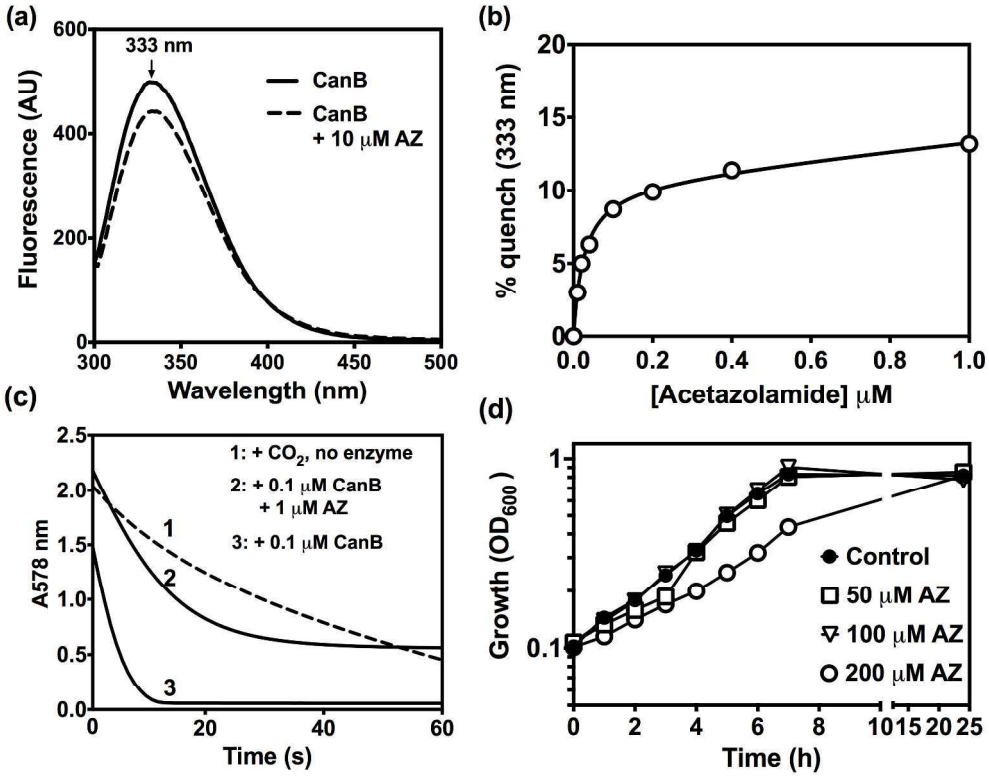

Figure 8
252x200mm (300 x 300 DPI)